# Masked SSL tasks for images

Ildus Sadrtdinov, 07.02.23

# Self-supervised pre-training

generative

discriminative

generative pre-text tasks

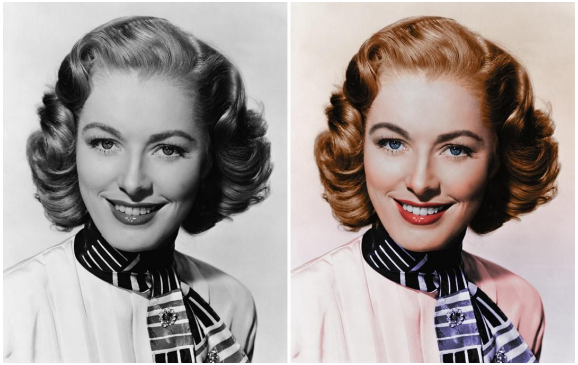

discriminative pre-text tasks

contrastive tasks

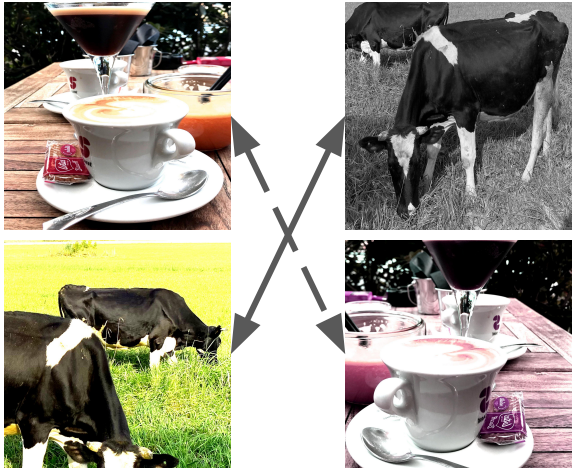

# Self-supervised pre-training

generative

discriminative

masked image modelling

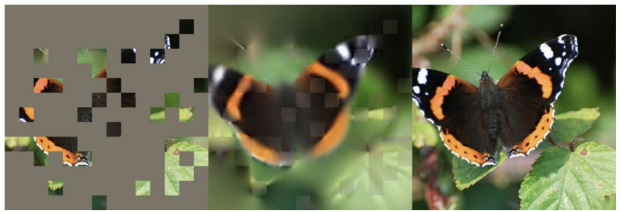

generative pre-text tasks

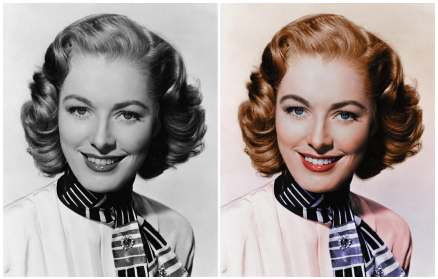

discriminative pre-text tasks

contrastive tasks

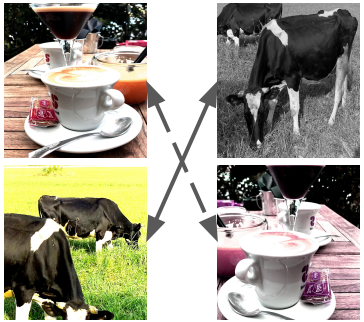

# Plan

- **Transformers for images**
  - ViT, DEiT
  - Self-distillation with no labels (DINO)
- **Masked Image Modeling**
  - BEiT, MAE
  - MaskFeat
- **Improving Contrastive Learning**
  - Distilling Localization (DiLo)
  - Leave-one-out Contrastive Learning (LooC)
  - Nearest-Neighbor Contrastive Learning (NNCLR)

# Plan

- **Transformers for images**
  - ViT, DEiT
  - Self-distillation with no labels (DINO)
- **Masked Image Modeling**
  - BEiT, MAE
  - MaskFeat
- **Improving Contrastive Learning**
  - Distilling Localization (DiLo)
  - Leave-one-out Contrastive Learning (LooC)
  - Nearest-Neighbor Contrastive Learning (NNCLR)

# Vision Transformer (ViT)

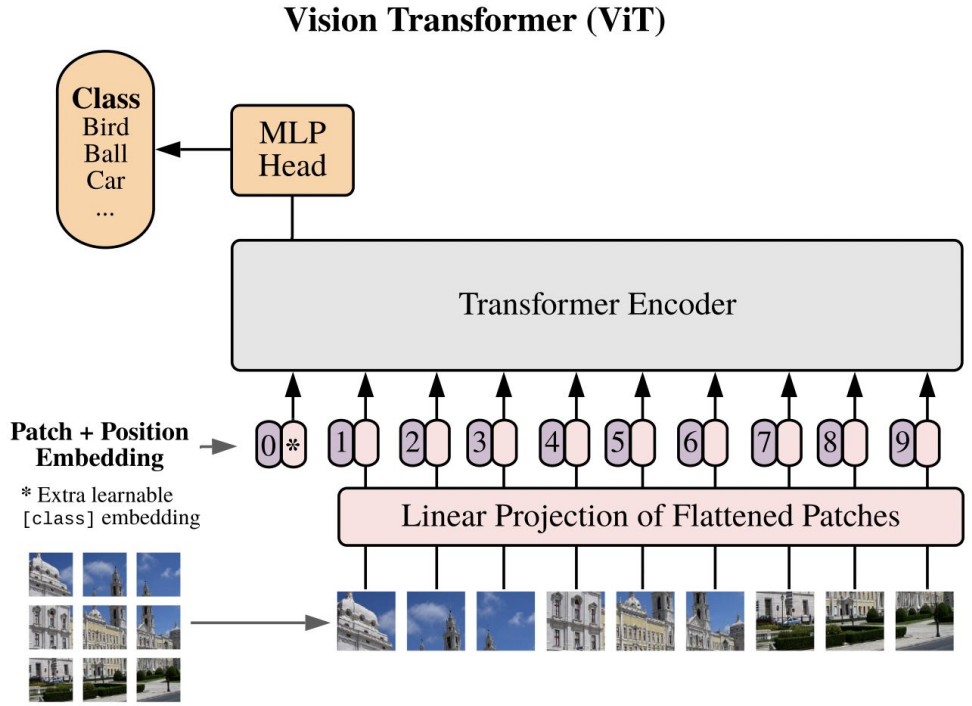


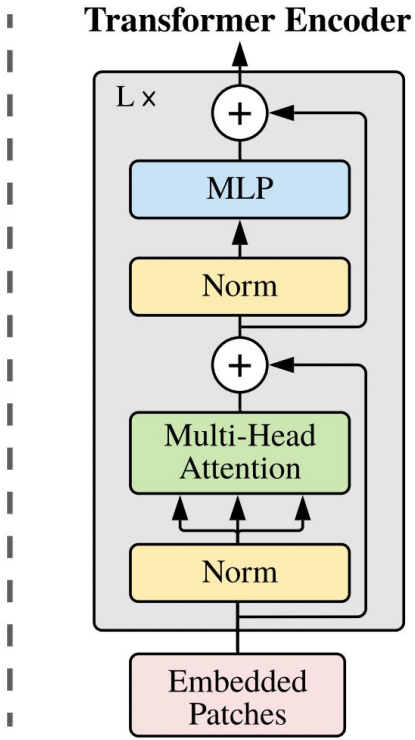


Dosovitskiy et al., 2021

# Vision Transformer (ViT)

However, ViT has significant drawbacks:

- ViT performs worse than ConvNets when trained from scratch on **medium-size datasets** (i.e. ImageNet-1K)
- ViT requires pre-training on **large datasets** (i.e. ImageNet-22K or JFT-300M)

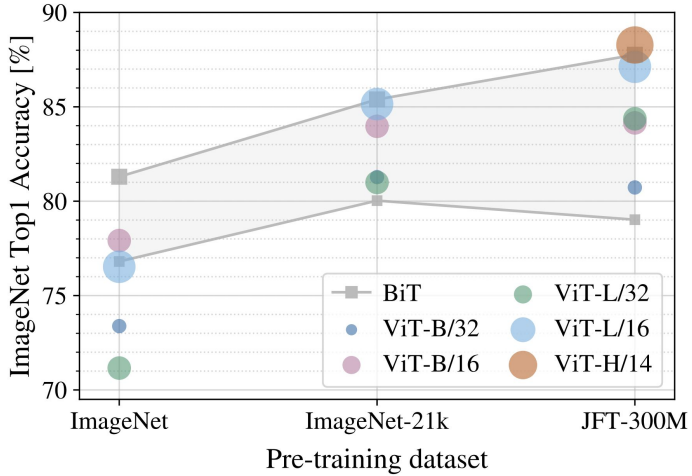


Dosovitskiy et al., 2021

# Data-Efficient Image Transformers (DEiT)

- Same architecture as ViT
- Distillation from a ConvNet teacher pre-trained on ImageNet (i.e. no external data)
- Special distillation token (similar to [CLS] token)

| method ↓ | Supervision label | Supervision teacher | ImageNet top-1 (%) Ti 224 | S 224 | B 224 | B↑384 |
|---|---|---|---|---|---|---|
| DeiT– no distillation | ✓ | ✗ | 72.2 | 79.8 | 81.8 | 83.1 |
| DeiT– usual distillation | ✗ | soft | 72.2 | 79.8 | 81.8 | 83.2 |
| DeiT– hard distillation | ✗ | hard | 74.3 | 80.9 | 83.0 | 84.0 |
| DeiT⚗: class embedding | ✓ | hard | 73.9 | 80.9 | 83.0 | 84.2 |
| DeiT⚗: distil. embedding | ✓ | hard | 74.6 | 81.1 | 83.1 | 84.4 |
| DeiT⚗: class+distillation | ✓ | hard | 74.5 | 81.2 | 83.4 | 84.5 |

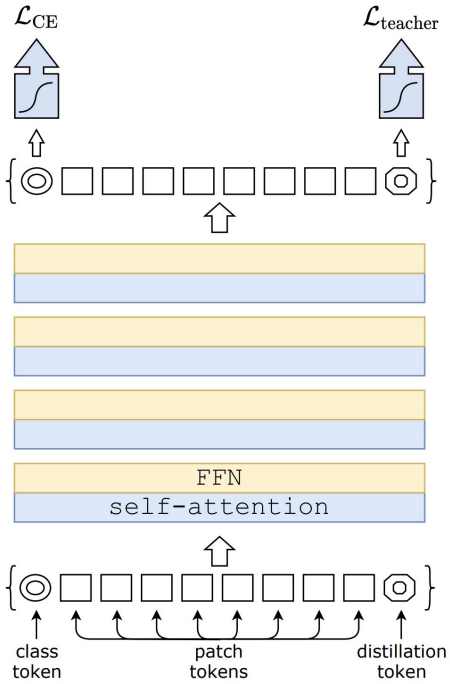


Touvron et al., 2021

# Emerging Properties in Self-Supervised Vision Transformers

FAIR

- Self-supervised ViT features contain explicit information about **semantic segmentation** (opposed to supervised ViTs and ConvNets)
- Self-supervised ViT features are **excellent k-NN classifiers**
- Importance of **momentum encoder**, **multi-crop training**, **small patches**
- **DINO** – self-**DI**stillation with **NO** labels (contrastive w/o negative examples)

Caron et al., 2021

# DINO: scheme

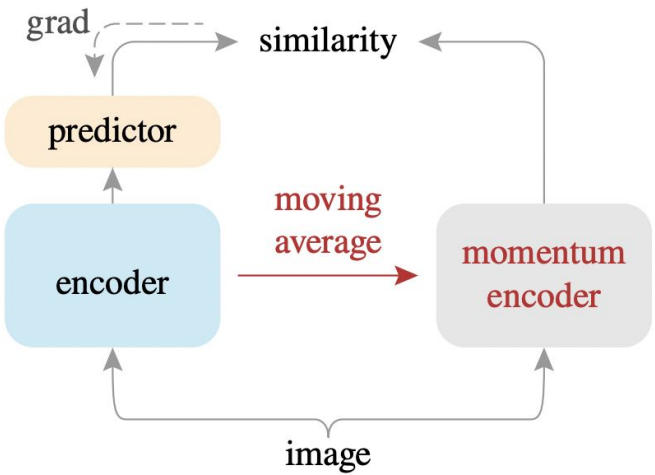


BYOL

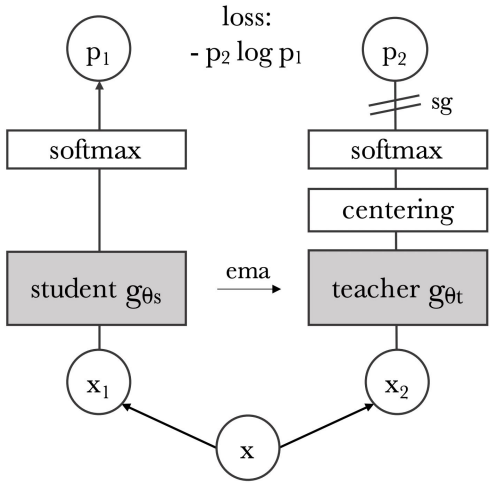


DINO

$$\mathcal{L} = -\sum_{k=1}^{K} p_k^t \log p_k^s$$

Caron et al., 2021

# DINO: avoiding collapse

## centering

$$g_{\theta_t}(x) \leftarrow g_{\theta_t}(x) - c$$

$$c \leftarrow mc + (1-m)\frac{1}{B}\sum_{i=1}^{B} g_{\theta_t}(x_i)$$

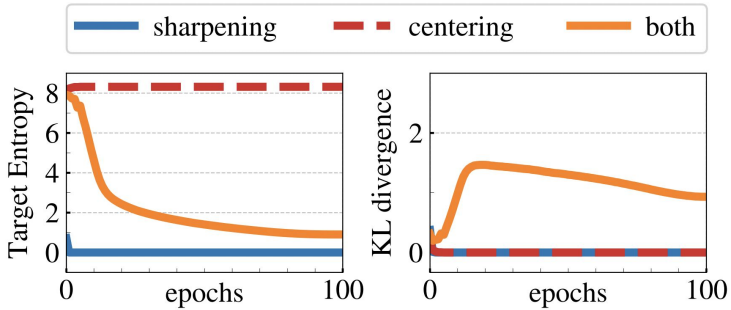


Figure 7: **Collapse study. (left)**: evolution of the teacher's target entropy along training epochs; **(right)**: evolution of KL divergence between teacher and student outputs.

## sharpening

$$p_t(x)^{(i)} = \frac{\exp(g_{\theta_t}(x)^{(i)}/\tau_t)}{\sum_{k=1}^{K}\exp(g_{\theta_t}(x)^{(k)}/\tau_t)}, 0 < \tau_t < 1$$

$$H(P_t, P_s) = h(P_t) + D_{KL}(P_t|P_s)$$

Caron et al., 2021

# DINO: comparison to contrastive methods (300ep, ViT-S/16)

| | Method | Mom. | SK | MC | Loss | Pred. | $k$-NN | Lin. |
|---|---|---|---|---|---|---|---|---|
| 1 | DINO | ✓ | ✗ | ✓ | CE | ✗ | 72.8 | 76.1 |
| 2 | | ✗ | ✗ | ✓ | CE | ✗ | 0.1 | 0.1 |
| 3 | | ✓ | ✓ | ✓ | CE | ✗ | 72.2 | 76.0 |
| 4 | | ✓ | ✗ | ✗ | CE | ✗ | 67.9 | 72.5 |
| 5 | | ✓ | ✗ | ✓ | MSE | ✗ | 52.6 | 62.4 |
| 6 | | ✓ | ✗ | ✓ | CE | ✓ | 71.8 | 75.6 |
| 7 | BYOL | ✓ | ✗ | ✗ | MSE | ✓ | 66.6 | 71.4 |
| 8 | MoCov2 | ✓ | ✗ | ✗ | INCE | ✗ | 62.0 | 71.6 |
| 9 | SwAV | ✗ | ✓ | ✓ | CE | ✗ | 64.7 | 71.8 |

SK: Sinkhorn-Knopp, MC: Multi-Crop, Pred.: Predictor
CE: Cross-Entropy, MSE: Mean Square Error, INCE: InfoNCE

Caron et al., 2021

# DINO: results

| Method | Arch. | Param. | im/s | Linear | $k$-NN |
|---|---|---|---|---|---|
| Supervised | RN50 | 23 | 1237 | 79.3 | 79.3 |
| SCLR [12] | RN50 | 23 | 1237 | 69.1 | 60.7 |
| MoCov2 [15] | RN50 | 23 | 1237 | 71.1 | 61.9 |
| InfoMin [67] | RN50 | 23 | 1237 | 73.0 | 65.3 |
| BarlowT [81] | RN50 | 23 | 1237 | 73.2 | 66.0 |
| OBoW [27] | RN50 | 23 | 1237 | 73.8 | 61.9 |
| BYOL [30] | RN50 | 23 | 1237 | 74.4 | 64.8 |
| DCv2 [10] | RN50 | 23 | 1237 | 75.2 | 67.1 |
| SwAV [10] | RN50 | 23 | 1237 | **75.3** | 65.7 |
| DINO | RN50 | 23 | 1237 | **75.3** | **67.5** |
| Supervised | ViT-S | 21 | 1007 | 79.8 | 79.8 |
| BYOL* [30] | ViT-S | 21 | 1007 | 71.4 | 66.6 |
| MoCov2* [15] | ViT-S | 21 | 1007 | 72.7 | 64.4 |
| SwAV* [10] | ViT-S | 21 | 1007 | 73.5 | 66.3 |
| DINO | ViT-S | 21 | 1007 | **77.0** | **74.5** |

| Method | Arch. | Param. | im/s | Linear | $k$-NN |
|---|---|---|---|---|---|
| *Comparison across architectures* | | | | | |
| SCLR [12] | RN50w4 | 375 | 117 | 76.8 | 69.3 |
| SwAV [10] | RN50w2 | 93 | 384 | 77.3 | 67.3 |
| BYOL [30] | RN50w2 | 93 | 384 | 77.4 | – |
| DINO | ViT-B/16 | 85 | 312 | 78.2 | 76.1 |
| SwAV [10] | RN50w5 | 586 | 76 | 78.5 | 67.1 |
| BYOL [30] | RN50w4 | 375 | 117 | 78.6 | – |
| BYOL [30] | RN200w2 | 250 | 123 | 79.6 | 73.9 |
| DINO | ViT-S/8 | 21 | 180 | 79.7 | **78.3** |
| SCLRv2 [13] | RN152w3+SK | 794 | 46 | 79.8 | 73.1 |
| DINO | ViT-B/8 | 85 | 63 | **80.1** | 77.4 |

Caron et al., 2021

# DINO: kNN for image retrieval & copy detection

Table 3: **Image retrieval.** We compare the performance in retrieval of off-the-shelf features pretrained with supervision or with DINO on ImageNet and Google Landmarks v2 (GLDv2) dataset. We report mAP on revisited Oxford and Paris. Pretraining with DINO on a landmark dataset performs particularly well. For reference, we also report the best retrieval method with off-the-shelf features [57].

| | | | $\mathcal{R}$Ox | | $\mathcal{R}$Par | |
|---|---|---|---|---|---|---|
| Pretrain | Arch. | Pretrain | M | H | M | H |
| Sup. [57] | RN101+R-MAC | ImNet | 49.8 | 18.5 | 74.0 | **52.1** |
| Sup. | ViT-S/16 | ImNet | 33.5 | 8.9 | 63.0 | 37.2 |
| DINO | ResNet-50 | ImNet | 35.4 | 11.1 | 55.9 | 27.5 |
| DINO | ViT-S/16 | ImNet | 41.8 | 13.7 | 63.1 | 34.4 |
| DINO | ViT-S/16 | GLDv2 | **51.5** | **24.3** | **75.3** | 51.6 |

Table 4: **Copy detection.** We report the mAP performance in copy detection on Copydays "strong" subset [21]. For reference, we also report the performance of the multigrain model [5], trained specifically for particular object retrieval.

| Method | Arch. | Dim. | Resolution | mAP |
|---|---|---|---|---|
| Multigrain [5] | ResNet-50 | 2048 | $224^2$ | 75.1 |
| Multigrain [5] | ResNet-50 | 2048 | largest side 800 | 82.5 |
| Supervised [69] | ViT-B/16 | 1536 | $224^2$ | 76.4 |
| DINO | ViT-B/16 | 1536 | $224^2$ | 81.7 |
| DINO | ViT-B/8 | 1536 | $320^2$ | **85.5** |

Caron et al., 2021

# DINO: attention maps to segmentation masks

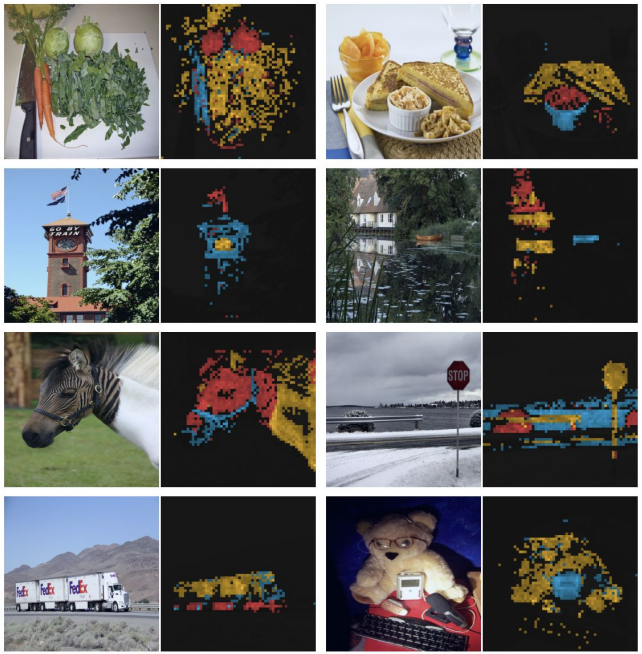

Figure 3: **Attention maps from multiple heads.** We consider the heads from the last layer of a ViT-S/8 trained with DINO and display the self-attention for `[CLS]` token query. Different heads, materialized by different colors, focus on different locations that represents different objects or parts (more examples in Appendix).

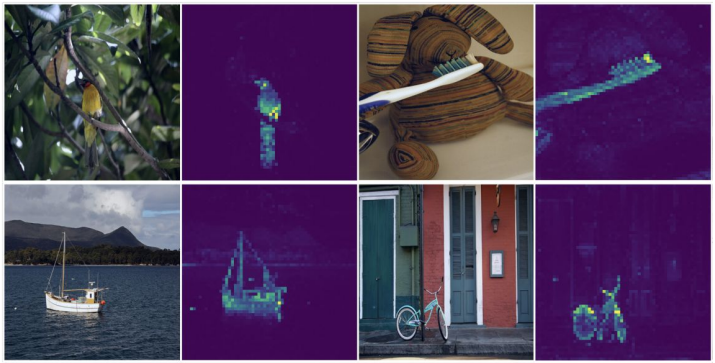

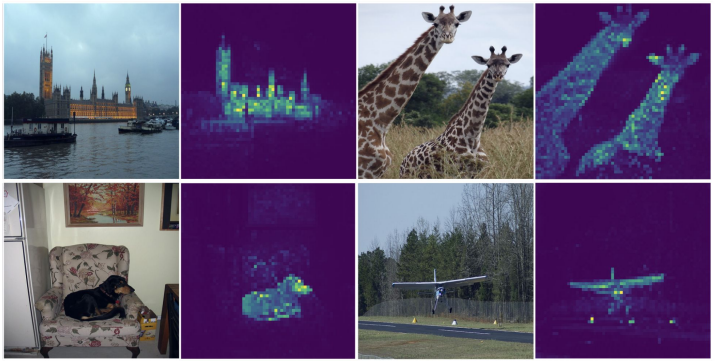

Caron et al., 2021

# DINO: attention maps to segmentation masks

| | Random | Supervised | DINO |
|---|---|---|---|
| ViT-S/16 | 22.0 | 27.3 | 45.9 |
| ViT-S/8 | 21.8 | 23.7 | 44.7 |

Figure 4: **Segmentations from supervised versus DINO.** We visualize masks obtained by thresholding the self-attention maps to keep 60% of the mass. On top, we show the resulting masks for a ViT-S/8 trained with supervision and DINO. We show the best head for both models. The table at the bottom compares the Jaccard similarity between the ground truth and these masks on the validation images of PASCAL VOC12 dataset.

*Supervised*

*DINO*

Caron et al., 2021

# DINO: ablations

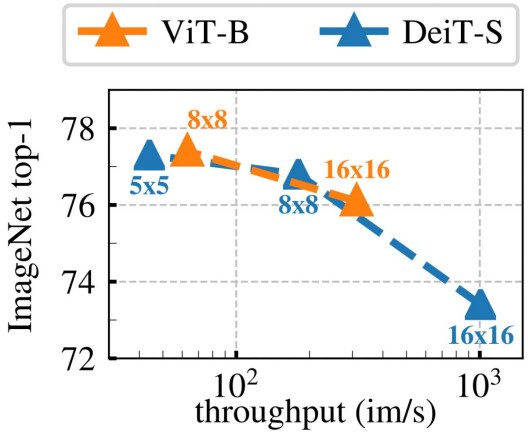


Figure 5: **Effect of Patch Size.** $k$-NN evaluation as a function of the throughputs for different input patch sizes with ViT-B and ViT-S. Models are trained for 300 epochs.

| bs | 128 | 256 | 512 | 1024 |
|---|---|---|---|---|
| top-1 | 57.9 | 59.1 | 59.6 | 59.9 |

Table 9: **Effect of batch sizes.** Top-1 with $k$-NN for models trained for 100 epochs without multi-crop.

Table 8: **Time and memory requirements.** We show total running time and peak memory per GPU ("mem.") when running ViT-S/16 DINO models on two 8-GPU machines. We report top-1 ImageNet val acc with linear evaluation for several variants of multi-crop, each having a different level of compute requirement.

| | 100 epochs | | 300 epochs | | |
|---|---|---|---|---|---|
| multi-crop | top-1 | time | top-1 | time | mem. |
| $2\times224^2$ | 67.8 | 15.3h | 72.5 | 45.9h | 9.3G |
| $2\times224^2 + 2\times96^2$ | 71.5 | 17.0h | 74.5 | 51.0h | 10.5G |
| $2\times224^2 + 6\times96^2$ | 73.8 | 20.3h | 75.9 | 60.9h | 12.9G |
| $2\times224^2 + 10\times96^2$ | 74.6 | 24.2h | 76.1 | 72.6h | 15.4G |

Caron et al., 2021

# Plan

- **Transformers for images**
  - ViT, DEiT
  - Self-distillation with no labels (DINO)
- **Masked Image Modeling**
  - BEiT, MAE
  - MaskFeat
- **Improving Contrastive Learning**
  - Distilling Localization (DiLo)
  - Leave-one-out Contrastive Learning (LooC)
  - Nearest-Neighbor Contrastive Learning (NNCLR)

# BEiT

**B**idirectional **E**ncoder representation from **I**mage **T**ransformers
Microsoft Research

- Masked Image Modeling (MIM) task
- Masking mechanism is similar to BERT
- Image is tokenized using dVAE and used as a target

Bao et al., 2021

# BEiT: scheme

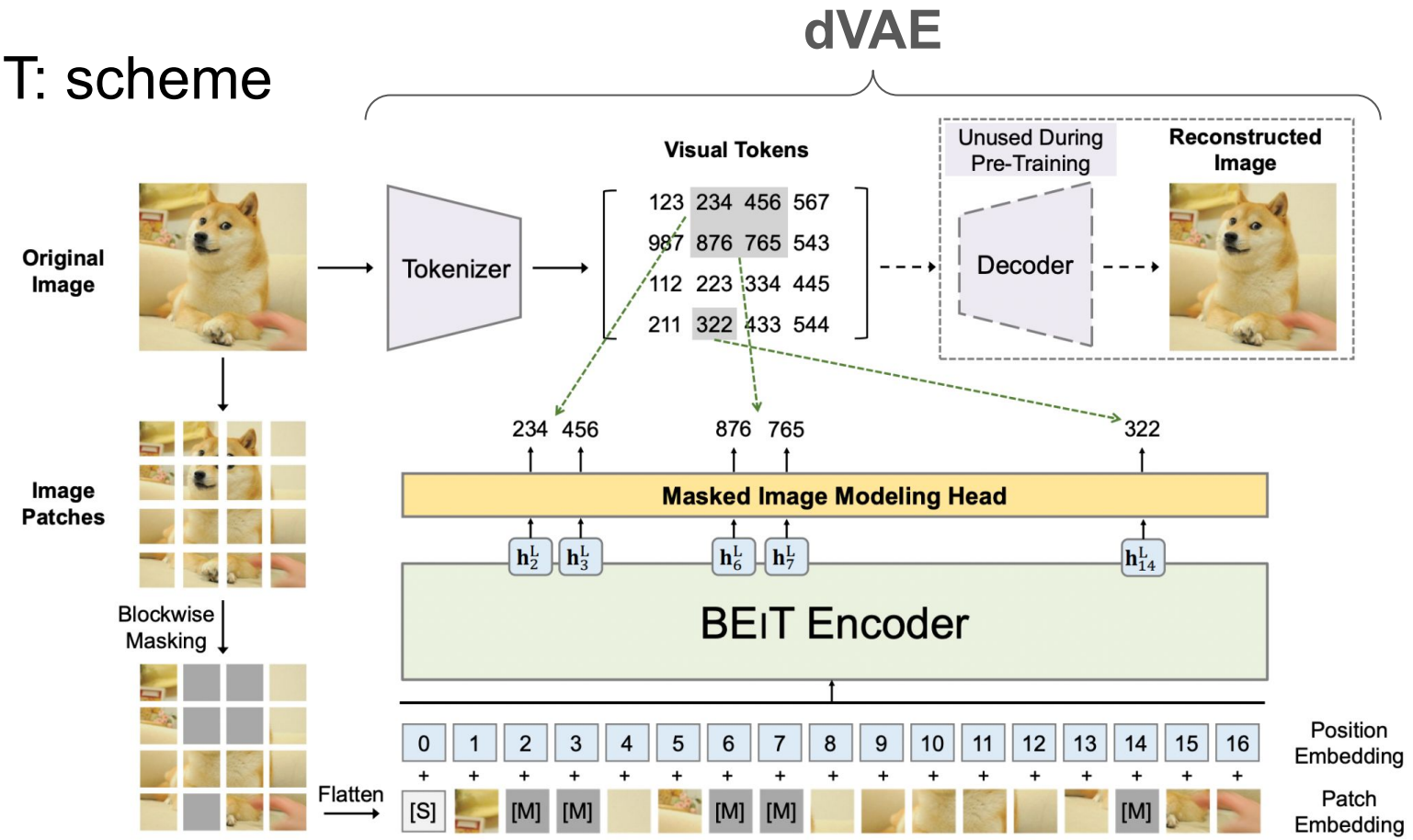


Bao et al., 2021

# BEiT: scheme

- 40% of patches are masked
- Masked patches are replaced with a learnable embedding
- Blockwise masking with a random aspect ratio and minimum 16 patches

**Algorithm 1** Blockwise Masking

**Input:** $N(= h \times w)$ image patches
**Output:** Masked positions $\mathcal{M}$
$\mathcal{M} \leftarrow \{\}$
**repeat**
  $s \leftarrow \text{Rand}(16, 0.4N - |\mathcal{M}|)$ ▷ *Block size*
  $r \leftarrow \text{Rand}(0.3, \frac{1}{0.3})$ ▷ *Aspect ratio of block*
  $a \leftarrow \sqrt{s \cdot r}; b \leftarrow \sqrt{s/r}$
  $t \leftarrow \text{Rand}(0, h - a)$ ; $l \leftarrow \text{Rand}(0, w - b)$
  $\mathcal{M} \leftarrow \mathcal{M} \bigcup \{(i, j) : i \in [t, t + a), j \in [l, l + b)\}$
**until** $|\mathcal{M}| > 0.4N$ ▷ *Masking ratio is* $40\%$
**return** $\mathcal{M}$

Bao et al., 2021

# BEiT: results

| Models | Model Size | Resolution | ImageNet |
|---|---|---|---|
| *Training from scratch (i.e., random initialization)* | | | |
| ViT$_{384}$-B [DBK+20] | 86M | $384^2$ | 77.9 |
| ViT$_{384}$-L [DBK+20] | 307M | $384^2$ | 76.5 |
| DeiT-B [TCD+20] | 86M | $224^2$ | 81.8 |
| DeiT$_{384}$-B [TCD+20] | 86M | $384^2$ | 83.1 |
| *Supervised Pre-Training on ImageNet-22K (using labeled data)* | | | |
| ViT$_{384}$-B [DBK+20] | 86M | $384^2$ | 84.0 |
| ViT$_{384}$-L [DBK+20] | 307M | $384^2$ | 85.2 |
| *Self-Supervised Pre-Training on ImageNet-1K (without labeled data)* | | | |
| iGPT-1.36B† [CRC+20] | 1.36B | $224^2$ | 66.5 |
| ViT$_{384}$-B-JFT300M‡ [DBK+20] | 86M | $384^2$ | 79.9 |
| MoCo v3-B [CXH21] | 86M | $224^2$ | 83.2 |
| MoCo v3-L [CXH21] | 307M | $224^2$ | 84.1 |
| DINO-B [CTM+21] | 86M | $224^2$ | 82.8 |
| BEiT-B (ours) | 86M | $224^2$ | 83.2 |
| BEiT$_{384}$-B (ours) | 86M | $384^2$ | 84.6 |
| BEiT-L (ours) | 307M | $224^2$ | 85.2 |
| BEiT$_{384}$-L (ours) | 307M | $384^2$ | **86.3** |

Table 1: Top-1 accuracy on ImageNet-1K. We evaluate base- ("-B") and large-size ("-L") models at resolutions 224 × 224 and 384 × 384. †: iGPT-1.36B contains 1.36 billion parameters, while others are base-size models. ‡: ViT$_{384}$-B-JFT300M is pretrained with the "masked patch prediction" task on Google's in-house 300M images, while others use ImageNet.

| Models | ADE20K |
|---|---|
| Supervised Pre-Training on ImageNet | 45.3 |
| DINO [CTM+21] | 44.1 |
| BEiT (ours) | 45.6 |
| BEiT + Intermediate Fine-Tuning (ours) | **47.7** |

Table 3: Results of semantic segmentation on ADE20K. We use SETR-PUP [ZLZ+20] as the task layer and report results of single-scale inference.

Bao et al., 2021

# BEiT: ablations

| Models | ImageNet | ADE20K |
|---|---|---|
| BEIT (300 Epochs) | 82.86 | 44.65 |
| − Blockwise masking | 82.77 | 42.93 |
| − Visual tokens (i.e., recover masked pixels) | 81.04 | 41.38 |
| − Visual tokens − Blockwise masking | 80.50 | 37.09 |
| + Recover 100% visual tokens | 82.59 | 40.93 |
| − Masking + Recover 100% visual tokens | 81.67 | 36.73 |
| Pretrain longer (800 epochs) | 83.19 | 45.58 |

Table 4: Ablation studies for BEIT pre-training on image classification and semantic segmentation.

- Directly using pixel-level auto-encoding pushes the model to focus on short-range dependencies and high-frequency details
- BEIT overcomes the above issue by predicting discrete visual tokens, which summarizes the details to high-level abstractions.

Bao et al., 2021

# BEiT: attention maps

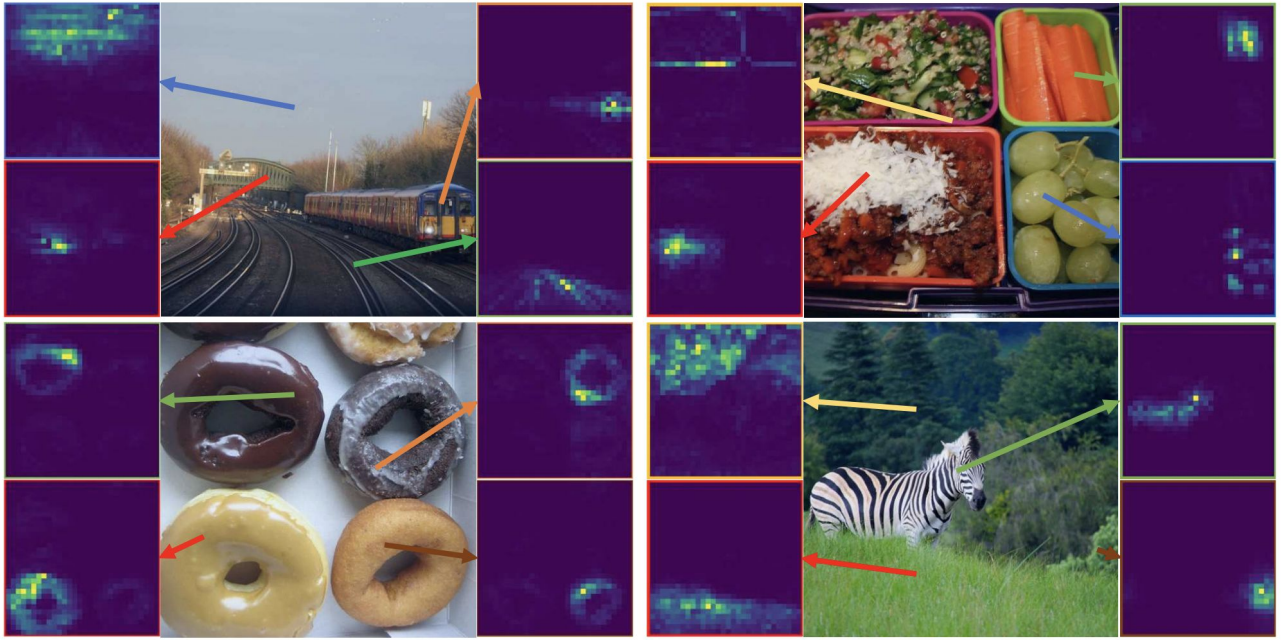

Figure 2: Self-attention map for different reference points. The self-attention mechanism in BEIT is able to separate objects, although self-supervised pre-training does not use manual annotations.

Bao et al., 2021

# MAE

**M**asked **A**uto**E**ncoders Are Scalable Vision Learners, FAIR

- Encoder-decoder architecture
- Encoder applied only to non-masked patches
- Mask high proportion (75%) of the input image
- Reconstruct images in the pixel space (i.e. not tokens as in BEiT), loss computed over masked patches only
- Decoder is flexible, smaller than encoder and takes both encodings of non-masked patches and mask tokens

He et al., 2021

# MAE: scheme

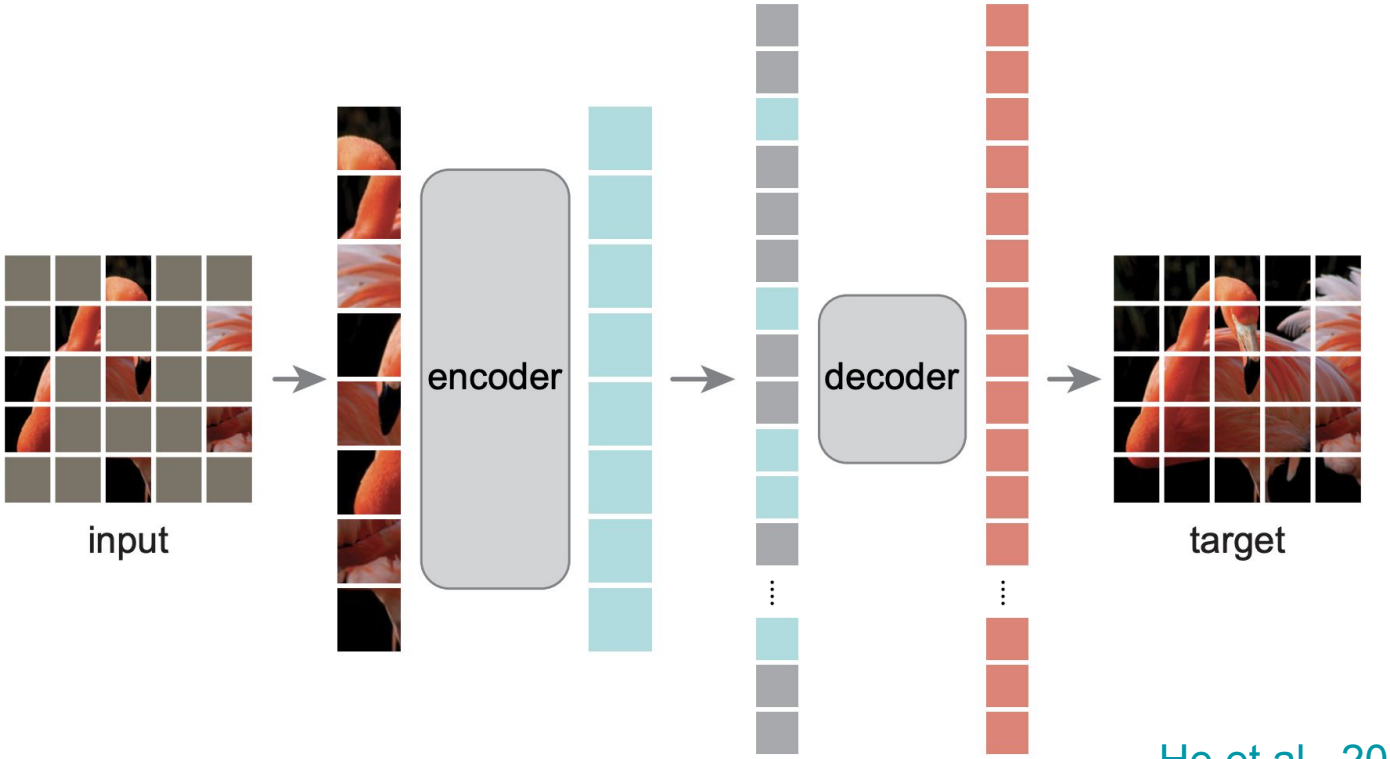


He et al., 2021

# MAE: reconstruction

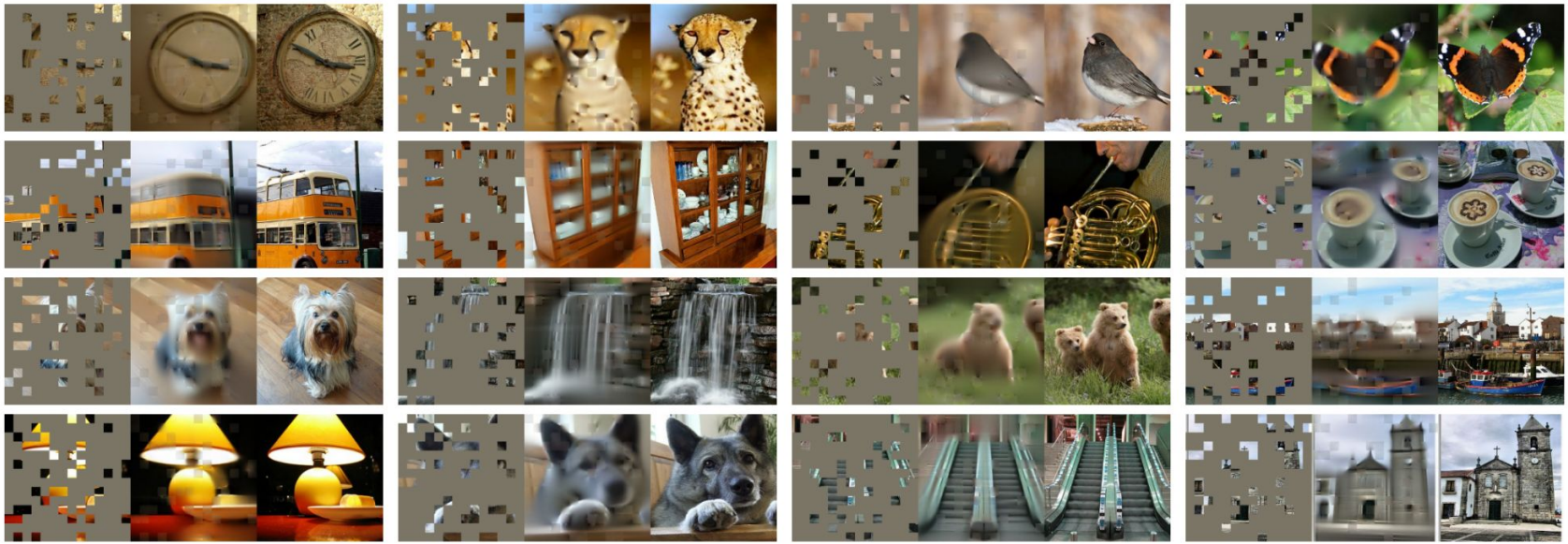

Figure 2. Example results on ImageNet *validation* images. For each triplet, we show the masked image (left), our MAE reconstruction† (middle), and the ground-truth (right). The masking ratio is 80%, leaving only 39 out of 196 patches. More examples are in the appendix.

†*As no loss is computed on visible patches, the model output on visible patches is qualitatively worse. One can simply overlay the output with the visible patches to improve visual quality. We intentionally opt not to do this, so we can more comprehensively demonstrate the method's behavior.*

He et al., 2021

# MAE: masking

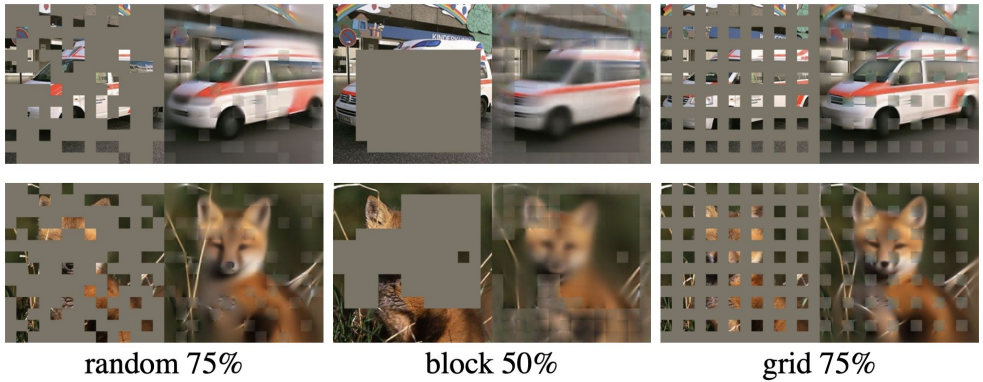


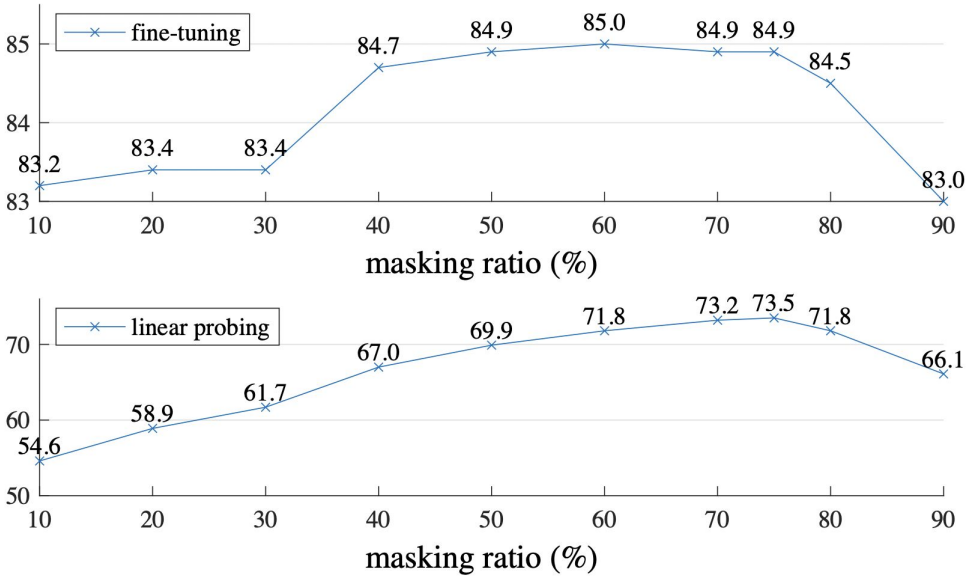


He et al., 2021

# MAE: ablations

| blocks | ft | lin |
|---|---|---|
| 1 | 84.8 | 65.5 |
| 2 | **84.9** | 70.0 |
| 4 | **84.9** | 71.9 |
| 8 | **84.9** | **73.5** |
| 12 | 84.4 | 73.3 |

(a) **Decoder depth**. A deep decoder can improve linear probing accuracy.

| dim | ft | lin |
|---|---|---|
| 128 | **84.9** | 69.1 |
| 256 | 84.8 | 71.3 |
| 512 | **84.9** | **73.5** |
| 768 | 84.4 | 73.1 |
| 1024 | 84.3 | 73.1 |

(b) **Decoder width**. The decoder can be narrower than the encoder (1024-d).

| case | ft | lin | FLOPs |
|---|---|---|---|
| encoder w/ [M] | 84.2 | 59.6 | 3.3× |
| encoder w/o [M] | **84.9** | **73.5** | **1**× |

(c) **Mask token**. An encoder without mask tokens is more accurate and faster (Table 2).

| case | ft | lin |
|---|---|---|
| pixel (w/o norm) | 84.9 | 73.5 |
| pixel (w/ norm) | **85.4** | **73.9** |
| PCA | 84.6 | 72.3 |
| dVAE token | 85.3 | 71.6 |

(d) **Reconstruction target**. Pixels as reconstruction targets are effective.

| case | ft | lin |
|---|---|---|
| none | 84.0 | 65.7 |
| crop, fixed size | 84.7 | 73.1 |
| crop, rand size | **84.9** | **73.5** |
| crop + color jit | 84.3 | 71.9 |

(e) **Data augmentation**. Our MAE works with minimal or no augmentation.

| case | ratio | ft | lin |
|---|---|---|---|
| random | 75 | **84.9** | **73.5** |
| block | 50 | 83.9 | 72.3 |
| block | 75 | 82.8 | 63.9 |
| grid | 75 | 84.0 | 66.0 |

(f) **Mask sampling**. Random sampling works the best. See Figure 6 for visualizations.

Table 1. **MAE ablation experiments** with ViT-L/16 on ImageNet-1K. We report fine-tuning (ft) and linear probing (lin) accuracy (%). If not specified, the default is: the decoder has depth 8 and width 512, the reconstruction target is unnormalized pixels, the data augmentation is random resized cropping, the masking ratio is 75%, and the pre-training length is 800 epochs. Default settings are marked in gray.

He et al., 2021

# MAE: results

| method | pre-train data | ViT-B | ViT-L | ViT-H | ViT-$H_{448}$ |
|---|---|---|---|---|---|
| scratch, our impl. | - | 82.3 | 82.6 | 83.1 | - |
| DINO [5] | IN1K | 82.8 | - | - | - |
| MoCo v3 [9] | IN1K | 83.2 | 84.1 | - | - |
| BEiT [2] | IN1K+DALLE | 83.2 | 85.2 | - | - |
| MAE | IN1K | 83.6 | 85.9 | 86.9 | **87.8** |

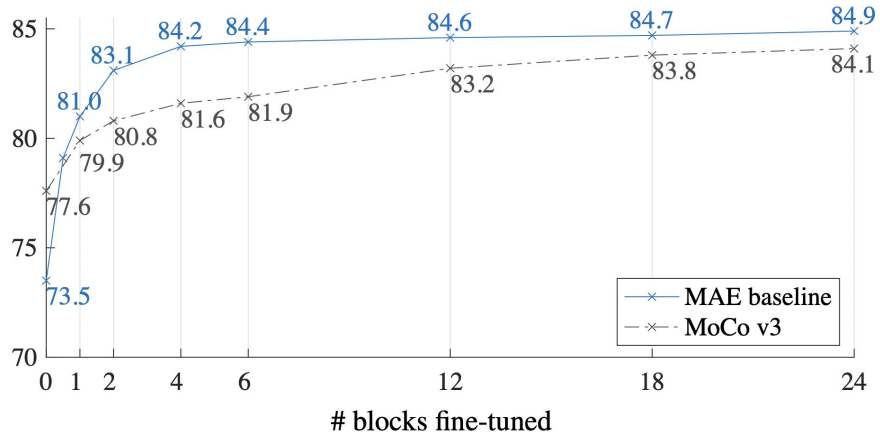


| | | $AP^{box}$ | | $AP^{mask}$ | |
|---|---|---|---|---|---|
| method | pre-train data | ViT-B | ViT-L | ViT-B | ViT-L |
| supervised | IN1K w/ labels | 47.9 | 49.3 | 42.9 | 43.9 |
| MoCo v3 | IN1K | 47.9 | 49.3 | 42.7 | 44.0 |
| BEiT | IN1K+DALLE | 49.8 | **53.3** | 44.4 | 47.1 |
| MAE | IN1K | **50.3** | **53.3** | **44.9** | **47.2** |

Table 4. **COCO object detection and segmentation** using a ViT Mask R-CNN baseline. All entries are based on our implementation. Self-supervised entries use IN1K data *without* labels. Mask AP follows a similar trend as box AP.

He et al., 2021

# MaskFeat

**Mask**ed **Feat**ure Prediction, FAIR

- Pre-training of video models
- Use features of masked patches (i.e. HOG) as a target for masked modelling

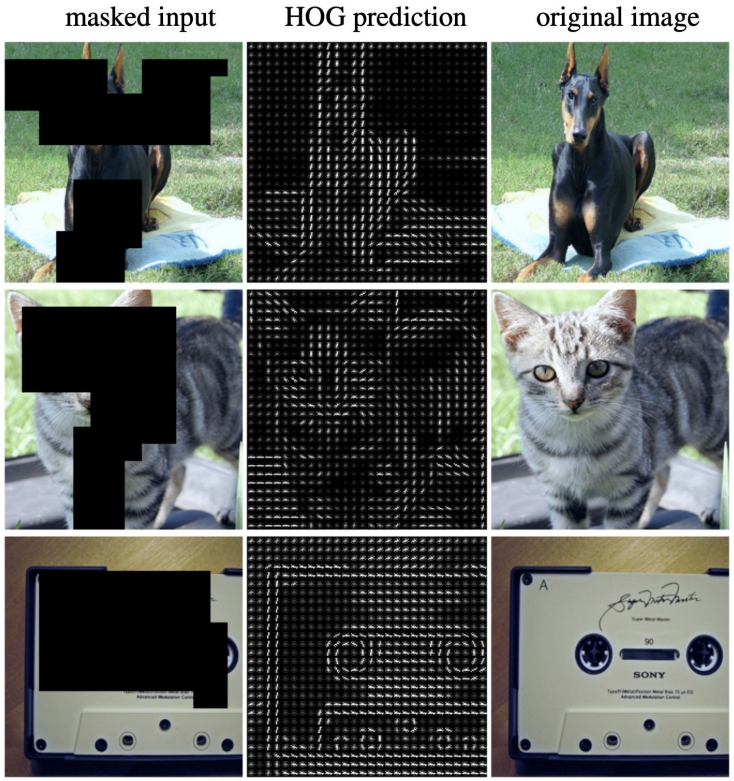


Wei et al., 2022

# Video Vision Transformer (ViViT)

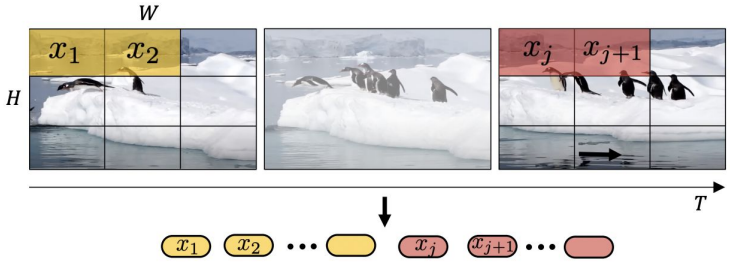


Figure 2: Uniform frame sampling: We simply sample $n_t$ frames, and embed each 2D frame independently following ViT [18].

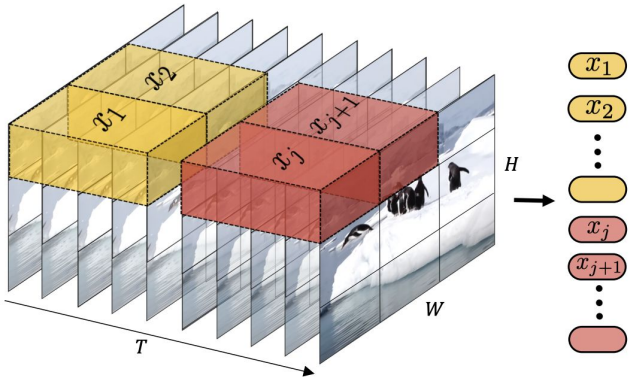


Figure 3: Tubelet embedding. We extract and linearly embed non-overlapping tubelets that span the spatio-temporal input volume.

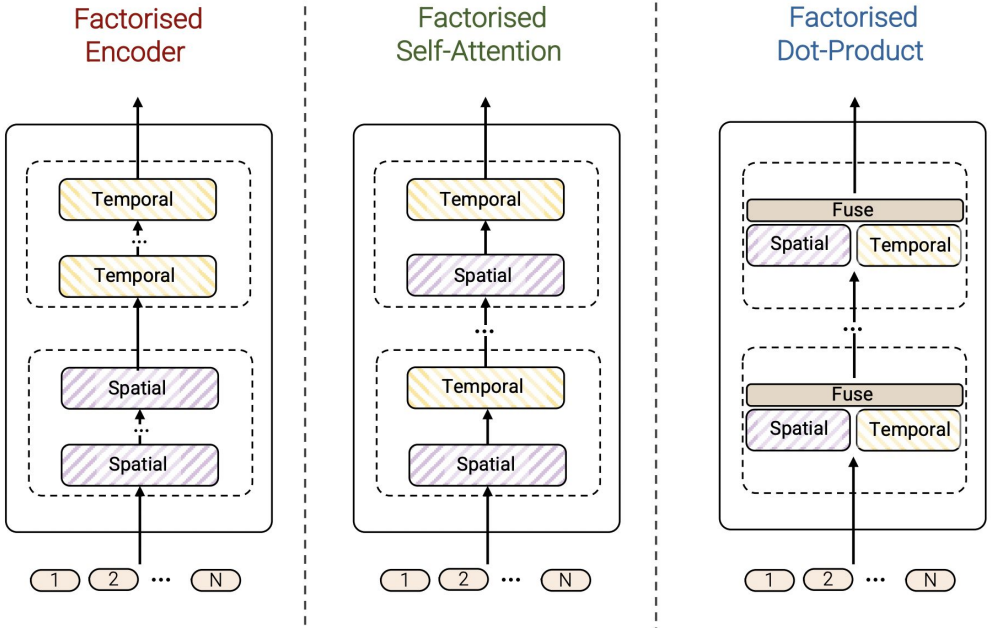


Arnab et al., 2021

# Multiscale Vision Transformer (MViT)

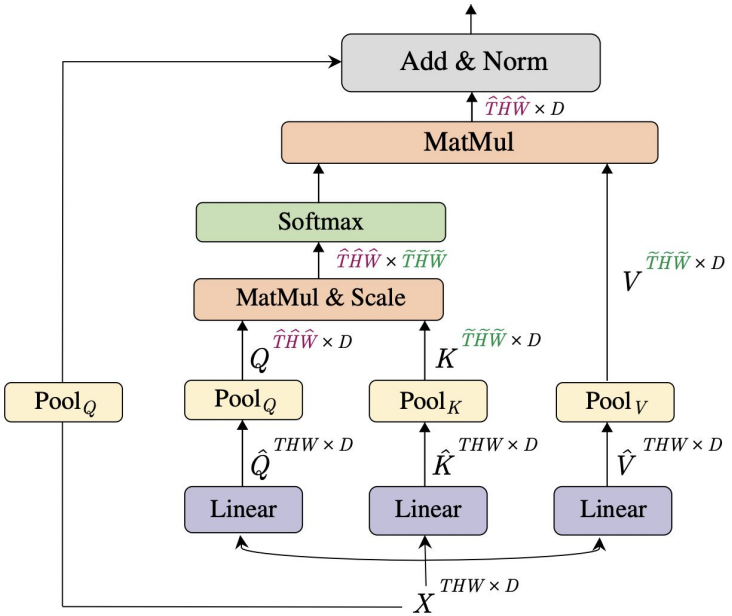


Figure 3. **Pooling Attention** is a flexible attention mechanism that (i) allows obtaining the reduced space-time resolution ($\hat{T}\hat{H}\hat{W}$) of the input ($THW$) by pooling the query, $Q = \mathcal{P}(\hat{Q}; \mathbf{\Theta}_Q)$, and/or (ii) computes attention on a reduced length ($\tilde{T}\tilde{H}\tilde{W}$) by pooling the key, $K = \mathcal{P}(\hat{K}; \mathbf{\Theta}_K)$, and value, $V = \mathcal{P}(\hat{V}; \mathbf{\Theta}_V)$, sequences.

| stages | operators | output sizes |
|---|---|---|
| data layer | stride $\tau \times 1 \times 1$ | $D \times T \times H \times W$ |
| $\text{cube}_1$ | $c_T \times c_H \times c_W$, $D$<br>stride $s_T \times 4 \times 4$ | $D \times \frac{T}{s_T} \times \frac{H}{4} \times \frac{W}{4}$ |
| $\text{scale}_2$ | $\begin{bmatrix} \text{MHPA}(D) \\ \text{MLP}(4D) \end{bmatrix} \times N_2$ | $D \times \frac{T}{s_T} \times \frac{H}{4} \times \frac{W}{4}$ |
| $\text{scale}_3$ | $\begin{bmatrix} \text{MHPA}(2D) \\ \text{MLP}(8D) \end{bmatrix} \times N_3$ | $2D \times \frac{T}{s_T} \times \frac{H}{8} \times \frac{W}{8}$ |
| $\text{scale}_4$ | $\begin{bmatrix} \text{MHPA}(4D) \\ \text{MLP}(16D) \end{bmatrix} \times N_4$ | $4D \times \frac{T}{s_T} \times \frac{H}{16} \times \frac{W}{16}$ |
| $\text{scale}_5$ | $\begin{bmatrix} \text{MHPA}(8D) \\ \text{MLP}(32D) \end{bmatrix} \times N_5$ | $8D \times \frac{T}{s_T} \times \frac{H}{32} \times \frac{W}{32}$ |

Fan et al., 2021

# MaskFeat: scheme & features

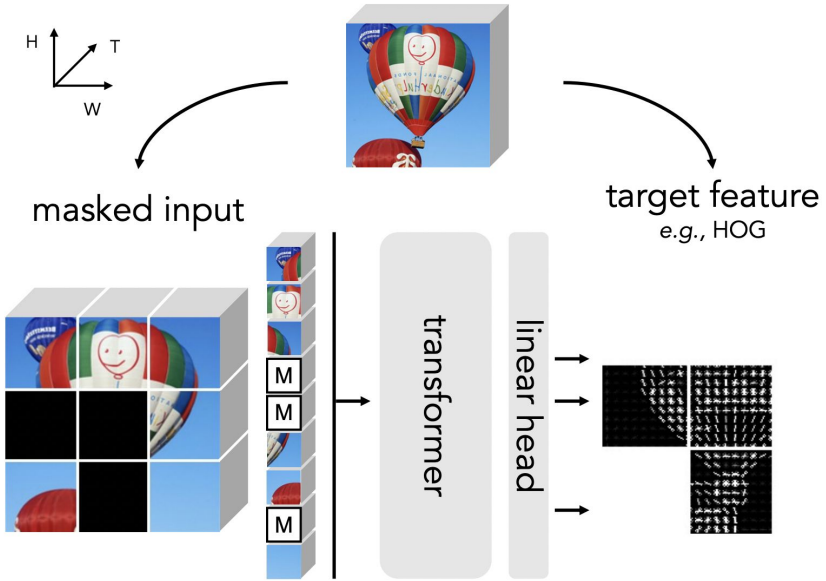


Figure 2. **MaskFeat pre-training.** We randomly replace the input space-time cubes of a video with a `[MASK]` token and directly regress features (*e.g.* HOG) of the masked regions. After pre-training, the Transformer is fine-tuned on end tasks.

| feature type | one-stage | variant | top-1 |
|---|---|---|---|
| scratch | - | MViTv2-S [46] | 81.1 |
| pixel | ✓ | RGB | 80.7 |
| image descriptor | ✓ | HOG [18] | **82.2** |
| dVAE | ✗ | DALL-E [58] | 81.7 |
| unsupervised feature | ✗ | DINO [9], ViT-B | **82.5** |
| supervised feature | ✗ | MViT-B [26] | 81.9 |

Table 1. **Comparing target features for MaskFeat (*video*).** All variants are pre-trained for 300 epochs on MViTv2-S, 16×4 with MaskFeat. We report fine-tuning top-1 on K400. Default is `gray`.

Wei et al., 2022

# MaskFeat: results

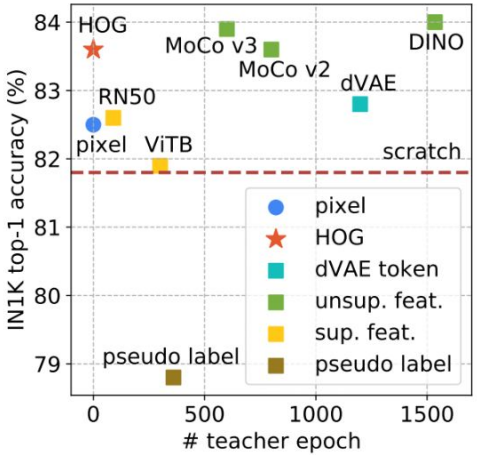


| feature type | one-stage | variant | arch. | param. | epoch† | top-1 |
|---|---|---|---|---|---|---|
| scratch | - | DeiT [63] | - | - | - | 81.8 |
| pixel colors | ✓ | RGB | - | - | - | 82.5 |
| image descriptor | ✓ | HOG [18] | - | - | - | **83.6** |
| dVAE token | ✗ | DALL-E [58] | dVAE | 54 | 1199 | 82.8 |
| unsupervised feature | ✗ | MoCo v2 [15] | ResNet50 | 23 | 800 | 83.6 |
| unsupervised feature | ✗ | MoCo v3 [17] | ViT-B | 85 | 600 | 83.9 |
| unsupervised feature | ✗ | DINO [9] | ViT-B | 85 | 1535 | **84.0** |
| supervised feature | ✗ | pytorch [53] | ResNet50 | 23 | 90 | 82.6 |
| supervised feature | ✗ | DeiT [63] | ViT-B | 85 | 300 | 81.9 |
| pseudo-label | ✗ | Token Labeling [42] | NFNet-F6 | 438 | 360 | 78.8 |

Table 2. **Comparing target features for MaskFeat (*image*).** For all targets, ViT-B is pre-trained with MaskFeat for 300 epochs on IN-1K. We report 100-epoch fine-tuning accuracy on IN-1K. For two-stage targets, we report the *teacher* architecture, number of parameters (M), and effective epoch† on IN-1K. The default entry is marked in gray. The plot on the left visualizes the acc/epoch trade-off of the table.

† Different teachers use different training strategies. dVAE is pre-trained on an external 250M dataset, while self-supervised methods require multi-view training. To measure the cost in a unified way, we normalize the number of epochs by the cost of one epoch on IN-1K training set with *one* $224^2$ *view*.

Wei et al., 2022

# MaskFeat: results

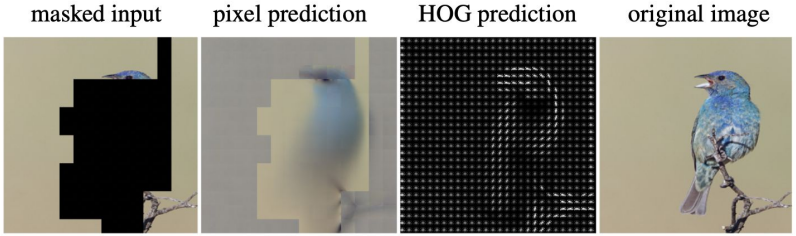


Both two predictions make good sense given a small visible region at the bird's head.

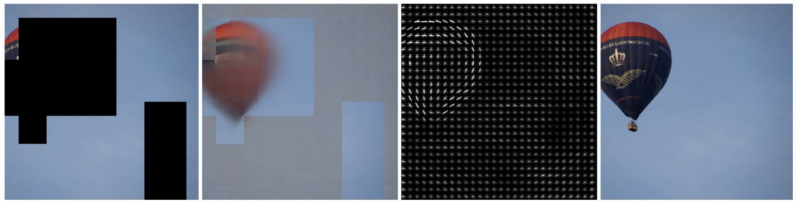

Pixel with **color ambiguity**: Though pixel prediction makes a sensible guess on the balloon, the loss penalty is large because of unmatched color (red *vs*. black).

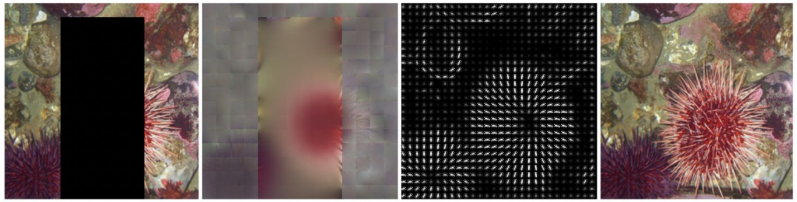

Pixel with **texture ambiguity**: Pixel prediction is blurry in texture-rich area because of ambiguity, while HOG successfully characterizes major edge directions.

| masking | frame | tube | cube |
|---|---|---|---|
| top-1 | 81.0 (-1.2) | 81.9 (-0.3) | **82.2** |

Table 6. **Masking strategy.** Varying the strategy of masking in spatiotemporal data. The default entry is highlighted in gray.

| pre-train | extra data | extra model | ViT-B | ViT-L |
|---|---|---|---|---|
| scratch [63] | - | - | 81.8 | 81.5 |
| supervised$_{384}$ [23] | IN-21K | - | 84.0 | 85.2 |
| MoCo v3 [17] | - | momentum ViT | 83.2 | 84.1 |
| DINO [9] | - | momentum ViT | 82.8 | - |
| BEiT [2] | DALL-E | dVAE | 83.2 | 85.2 |
| **MaskFeat** (w/ HOG) | - | - | **84.0** | **85.7** |

Table 7. **Comparison with previous work on IN-1K.** All entries are pre-trained on IN-1K train split, except supervised$_{384}$ using IN-21K. MoCo v3 and DINO use momentum encoder. BEiT uses 250M DALL-E data to pre-train dVAE. All entries are trained and evaluated at image size $224^2$ except supervised$_{384}$ at $384^2$.

Wei et al., 2022

# Plan

- **Transformers for images**
  - ViT, DEiT
  - Self-distillation with no labels (DINO)
- **Masked Image Modeling**
  - BEiT, MAE
  - MaskFeat
- **Improving Contrastive Learning**
  - Distilling Localization (DiLo)
  - Leave-one-out Contrastive Learning (LooC)
  - Nearest-Neighbor Contrastive Learning (NNCLR)

# DiLo

**Di**stilling **Lo**calization, Microsoft Research

- Self-supervised ConvNets are bad at localizing object in the image
- Main idea: force invariance to backgrounds
- Use saliency masks to cut object from the image and swap background

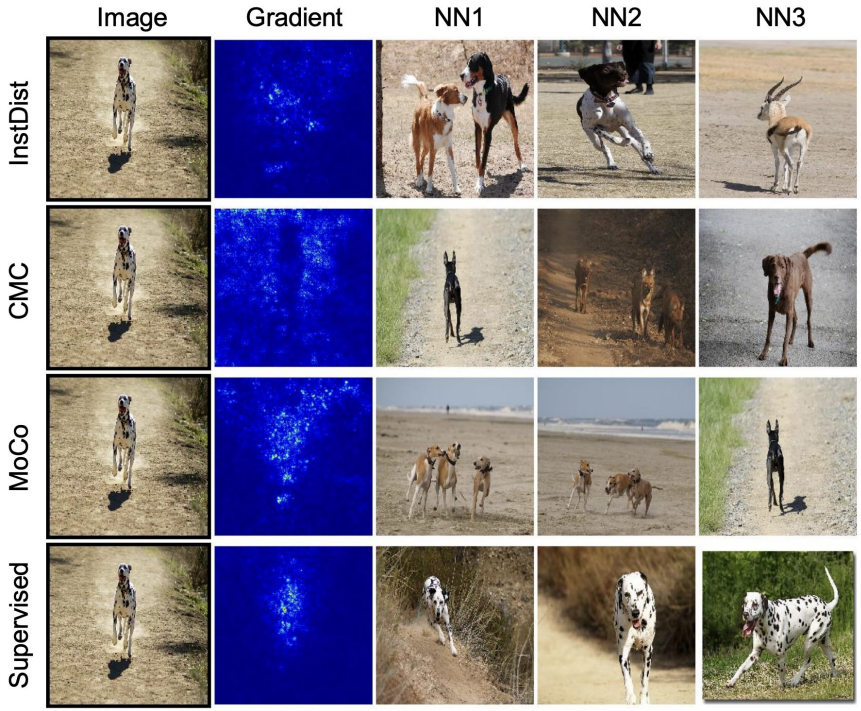


Zhao et al., 2020

# DiLo: saliency masks

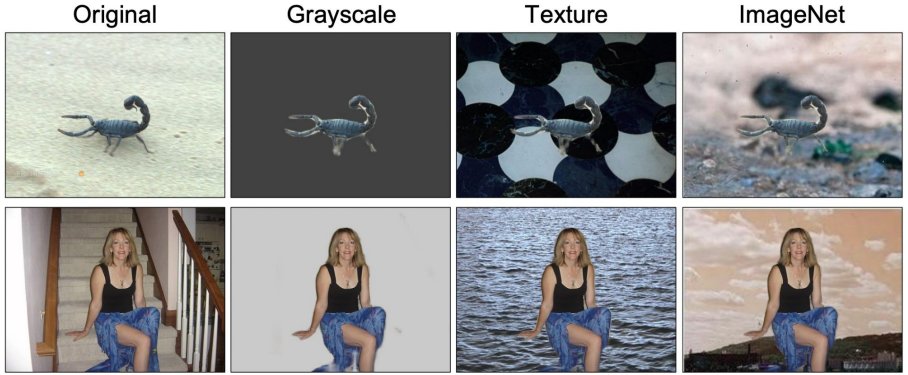


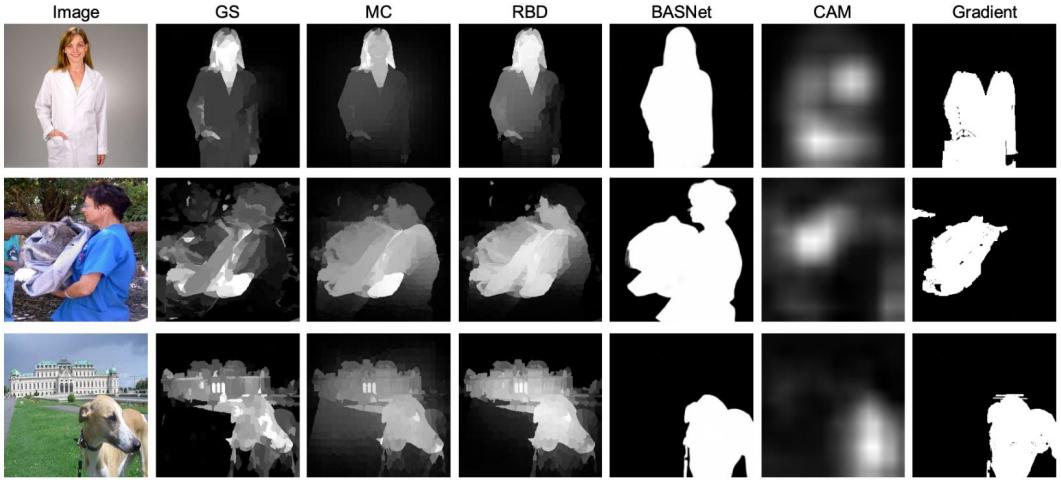


Figure 3: Examples of saliency estimations methods. We show 6 saliency estimations, including traditional methods (GS (Wei et al. 2012), MC (Jiang et al. 2013a), RBD (Zhu et al. 2014)), a network predicted saliency BASNet (Qin et al. 2019), and class-specific methods visualized from a pretrained network (CAM (Zhou et al. 2016), Gradient (Simonyan, Vedaldi, and Zisserman 2013)).

Zhao et al., 2020

# DiLo: ablations

Table 2: Ablation studies for investigating copy-and-pasting augmentations: (a) on various saliency estimation methods (b) on controlling the ratio of using copy-and-pasting augmentation (c) on various background images (d) on blending options.

(a)

| Saliency | $F_\beta$ | MAE | Acc | Δ |
|---|---|---|---|---|
| MoCo | - | - | 60.6 | - |
| GS | 0.557 | 0.173 | 62.7 | +2.1 |
| MC | 0.627 | 0.186 | 62.1 | +1.5 |
| RBD | 0.630 | 0.144 | 62.8 | +2.2 |
| BASNet | 0.805 | 0.056 | 65.0 | +4.4 |

(b)

| Aug Ratio | Linear | Δ |
|---|---|---|
| MoCo | 60.6 | - |
| 30% | 62.8 | +2.2 |
| 50% | 62.2 | +1.6 |
| 70% | 61.6 | +1.0 |
| 100% | 47.6 | -13.0 |

(c)

| Background | Linear | Δ |
|---|---|---|
| MoCo | 60.6 | - |
| Texture | 60.6 | +0.0 |
| Imagenet | 62.1 | +1.5 |
| Grayscale | 62.8 | +2.2 |

(d)

| Blending | Linear | Δ |
|---|---|---|
| MoCo | 60.6 | - |
| No blend | 62.4 | +1.8 |
| Gaussian | 62.5 | +1.9 |
| Mix | 62.8 | +2.2 |

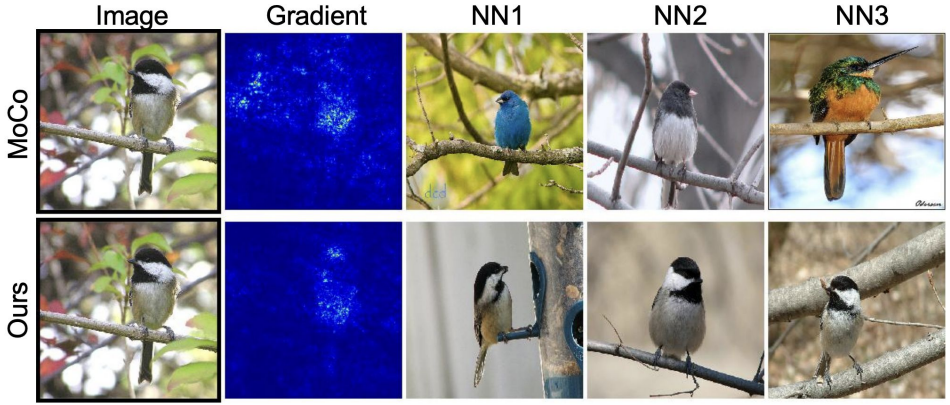


Zhao et al., 2020

# DiLo: results

Table 3: Distilling localization on various contrastive representation learning models for ImageNet classification.

| Methods | Original | DiLo-RBD | DiLo-BasNet |
|---|---|---|---|
| InstDist | 56.5 | 59.3 | 62.9 |
| CMC | 63.4 | 65.0 | 66.9 |
| MoCo-v1 | 60.6 | 62.8 | 65.0 |
| MoCo-v2 | 67.5 | 67.9 | 69.2 |

Table 4: Transfer learning for object detection on VOC 0712. We present the gap to ImageNet supervised pre-training in the brackets for reference. All numbers are the averages of three independent runs.

| Method | $AP$ | | $AP_{50}$ | | $AP_{75}$ | |
|---|---|---|---|---|---|---|
| Supervised | 53.5 | - | 81.3 | - | 58.8 | - |
| MoCo | 55.9 | (+2.4) | 81.5 | (+0.2) | 62.6 | (+3.8) |
| DiLo-RBD | 56.5 | (+3.0) | 81.9 | (+0.6) | 63.3 | (+4.5) |
| DiLo-BasNet | 56.9 | (+3.4) | 82.1 | (+0.8) | 64.1 | (+5.3) |

Table 5: Transfer learning for object detection and instance segmentation on COCO. Model is finetuned with Mask-RCNN ResNet50-FPN pipeline and 1x schedule.

| Method | $AP^{bb}$ | $AP^{bb}_{50}$ | $AP^{bb}_{75}$ | $AP^{mk}$ | $AP^{mk}_{50}$ | $AP^{mk}_{75}$ |
|---|---|---|---|---|---|---|
| Supervised | 39.7 | 59.5 | 43.3 | 35.9 | 56.6 | 38.6 |
| MoCo | 39.4 | 59.1 | 42.9 | 35.6 | 56.2 | 38.0 |
| DiLo-RBD | 39.8 | 59.5 | 43.3 | 36.0 | 56.7 | 38.6 |
| DiLo-BasNet | 40.1 | 60.0 | 44.0 | 36.3 | 56.8 | 39.0 |

Zhao et al., 2020

# What should not be contrastive in contrastive learning

Leave-one-out Contrastive Learning (LooC)

- Contrastive models are trained to force invariance over augmentations
- This invariance may be beneficial to one task and harmful to the other task
- Main idea: multi-head network with different embedding spaces, each forcing invariance over a single augmentation type

Xiao et al., 2020

# LooC: augmentation invariance

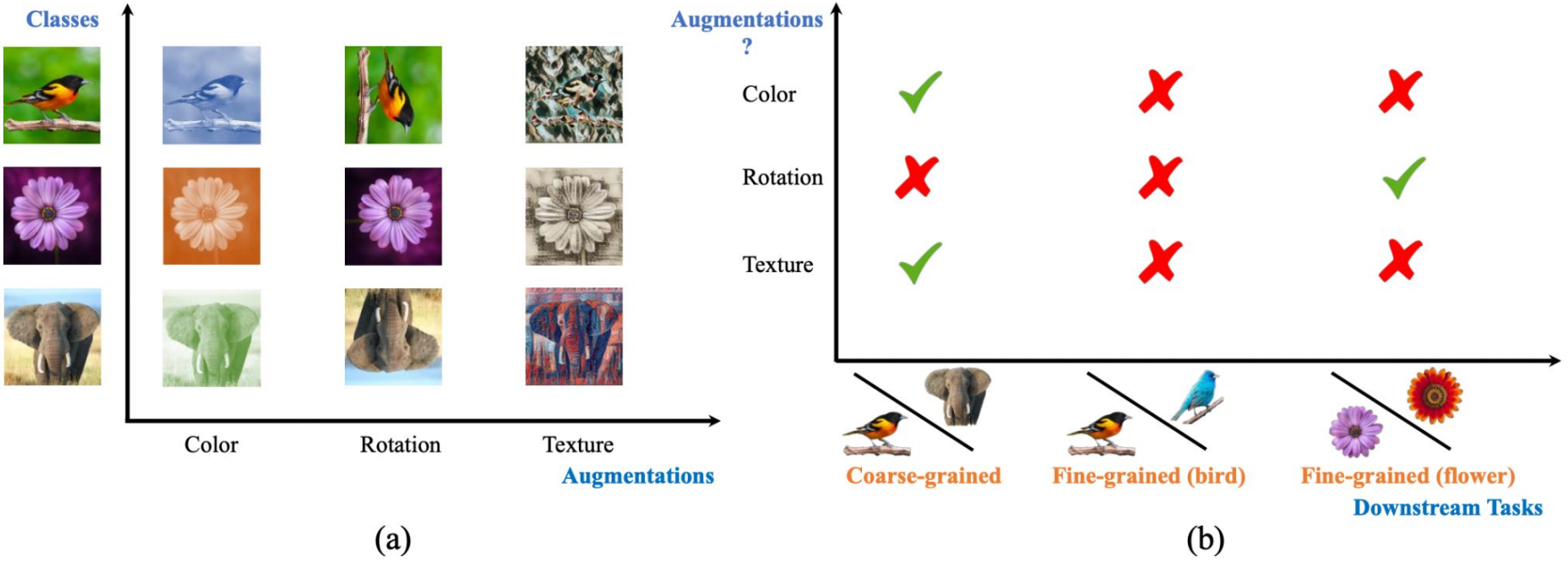


Xiao et al., 2020

# LooC: scheme

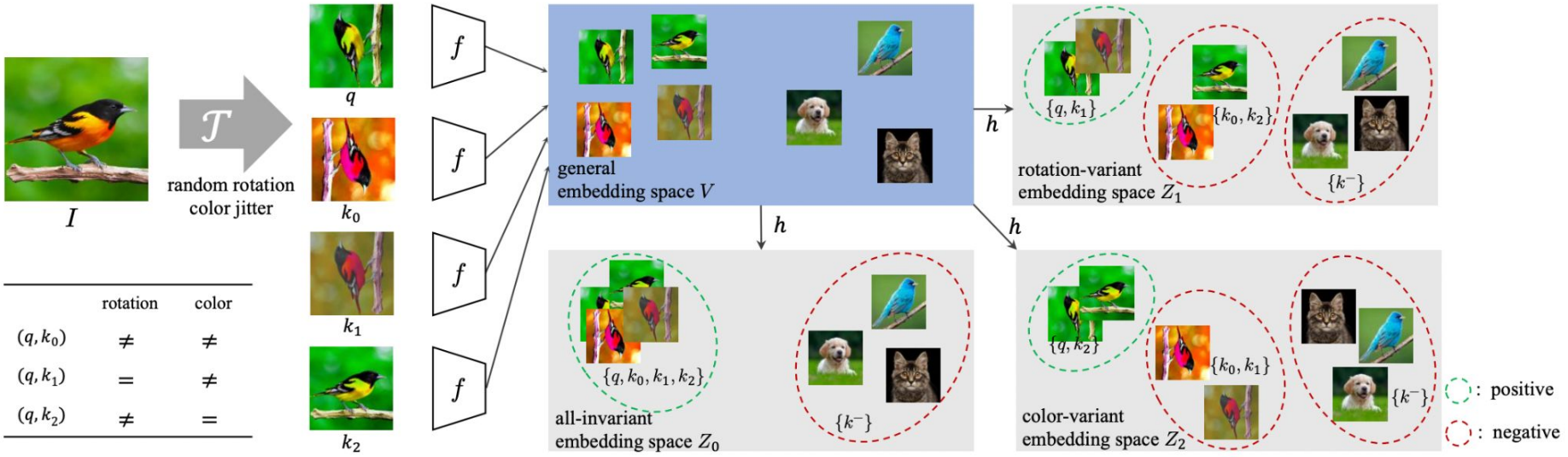


| | rotation | color |
|---|---|---|
| $(q, k_0)$ | $\neq$ | $\neq$ |
| $(q, k_1)$ | $=$ | $\neq$ |
| $(q, k_2)$ | $\neq$ | $=$ |

[Xiao et al., 2020]

# LooC: results

| model | Rotation Acc. | IN-100 top-1 | IN-100 top-5 |
|---|---|---|---|
| Supervised | 72.3 | 83.7 | 95.7 |
| MoCo | 61.1 | 81.0 | 95.2 |
| MoCo + Rotation | 43.3 | 79.4 | 94.1 |
| MoCo + Rotation (same for $q$ and $k$) | 45.5 | 78.1 | 94.3 |
| LooC + Rotation [ours] | 65.2 | 80.2 | 95.5 |

| model | Augmentation Color | Augmentation Rotation | iNat-1k top-1 | iNat-1k top-5 | CUB-200 top-1 | CUB-200 top-5 | Flowers-102 5-shot | Flowers-102 10-shot | IN-100 top-1 | IN-100 top-5 |
|---|---|---|---|---|---|---|---|---|---|---|
| MoCo | ✓ | | 36.2 | 62.0 | 36.7 | 64.7 | 67.9 ($\pm$ 0.5) | 77.3 ($\pm$ 0.1) | 81.0 | 95.2 |
| LooC | ✓ | | 41.2 | 67.0 | 40.1 | 69.7 | 68.2 ($\pm$ 0.6) | 77.6 ($\pm$ 0.1) | 81.1 | 95.3 |
| | | ✓ | 40.0 | 65.4 | 38.8 | 67.0 | 70.1 ($\pm$ 0.4) | 79.3 ($\pm$ 0.1) | 80.2 | 95.5 |
| | ✓ | ✓ | 44.0 | 69.3 | 39.6 | 69.2 | 70.9 ($\pm$ 0.3) | 80.8 ($\pm$ 0.2) | 79.2 | 94.7 |
| LooC++ | ✓ | ✓ | 46.1 | 71.5 | 39.3 | 69.3 | 68.1 ($\pm$ 0.4) | 78.8 ($\pm$ 0.2) | 81.2 | 95.2 |

Xiao et al., 2020

# NNCLR

**N**earest-**N**eighbor **C**ontrastive **L**earning of Visual **R**epresentations

- Use nearest neighbors in the latent space as positive examples for contrastive loss
- Nearest neighbors are search in a support set – an analogue for support set
- Resulting model is less sensitive to the choice of augmentations

Dwibedi et al., 2021

# NNCLR: scheme

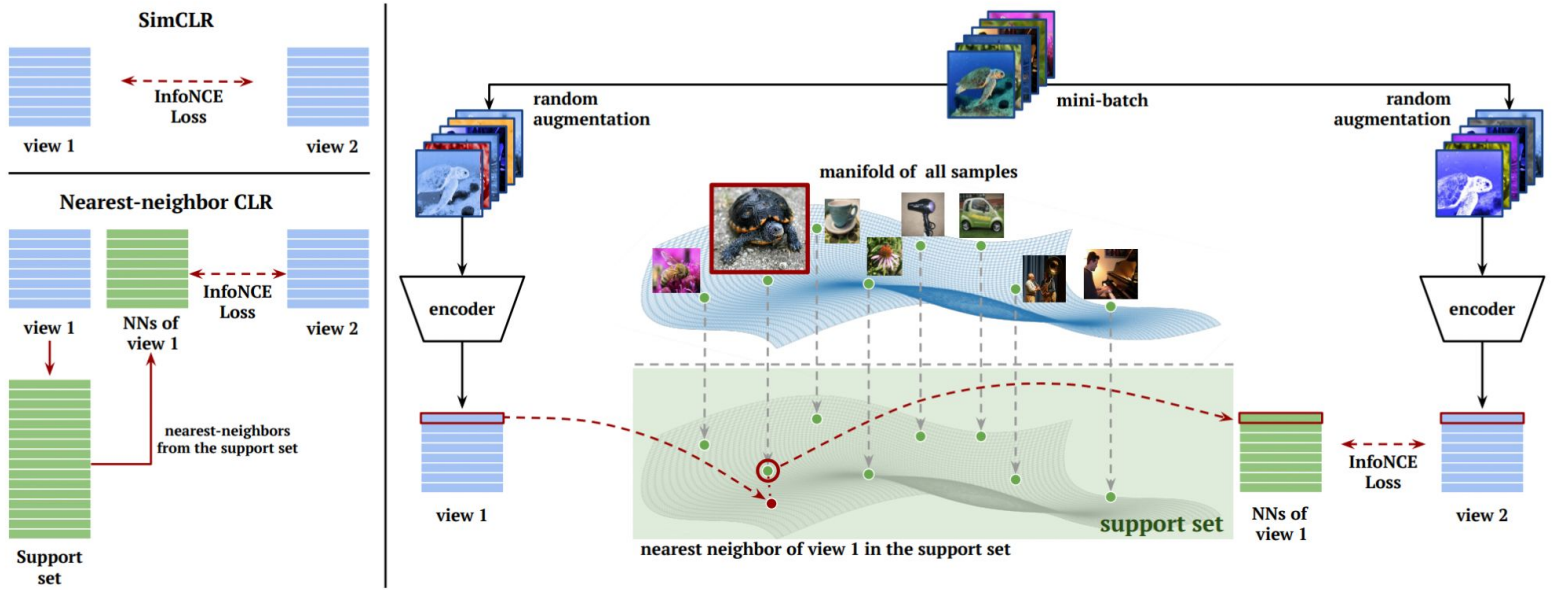


Figure 2: **Overview of NNCLR Training**

$$\mathcal{L}_i^{\text{NNCLR}} = -\log \frac{\exp\left(\text{NN}(z_i, Q) \cdot z_i^+ / \tau\right)}{\sum_{k=1}^{n} \exp\left(\text{NN}(z_i, Q) \cdot z_k^+ / \tau\right)}$$

$$\text{NN}(z, Q) = \underset{q \in Q}{\arg\min} \, \|z - q\|_2$$

Dwibedi et al., 2021

# NNCLR: results

| Method | Top-1 | Top-5 |
|---|---|---|
| PIRL [41] | 63.6 | - |
| CPC v2 [32] | 63.8 | 85.3 |
| PCL [39] | 65.9 | - |
| CMC [50] | 66.2 | 87.0 |
| MoCo v2 [11] | 71.1 | - |
| SimSiam [12] | 71.3 | - |
| SimCLR v2 [10] | 71.7 | - |
| SwAV [7] | 71.8 | N/A |
| InfoMin Aug. [51] | 73.0 | 91.1 |
| BYOL [25] | 74.3 | 91.6 |
| NNCLR (ours) | **75.4** | **92.3** |
| SwAV (multi-crop) [7] | 75.3 | N/A |
| NNCLR (ours) (multi-crop) | **75.6** | **92.4** |

Table 1: **ImageNet linear evaluation results.** Comparison with other self-supervised learning methods on ResNet-50 encoder. Methods on the top section use two views only.

| Method | ImageNet **1%** Top-1 | ImageNet **1%** Top-5 | ImageNet **10%** Top-1 | ImageNet **10%** Top-5 |
|---|---|---|---|---|
| Supervised | 25.4 | 48.4 | 56.4 | 80.4 |
| InstDisc [54] | - | 39.2 | - | 77.4 |
| PIRL [41] | - | 57.2 | - | 83.8 |
| PCL [39] | - | 75.6 | - | 86.2 |
| SimCLR [9] | 48.3 | 75.5 | 65.6 | 87.8 |
| BYOL [25] | 53.2 | 78.4 | 68.8 | 89.0 |
| NNCLR (ours) | **56.4** | **80.7** | **69.8** | **89.3** |
| SwAV (multi-crop) [7] | 53.9 | 78.5 | 70.2 | 89.9 |

Table 2: **Semi-supervised learning results on ImageNet.** Top-1 and top-5 performances are reported on fine-tuning a pre-trained ResNet-50 with ImageNet 1% and 10% datasets.

Dwibedi et al., 2021

# NNCLR: ablations

| Mom. Enc. | Positive | Top-1 | Top-5 |
|---|---|---|---|
| | View 1 | 71.4 | 90.4 |
| | NN of View 1 | **74.5** | **91.9** |
| ✓ | View 1 | 72.5 | 91.3 |
| ✓ | NN of View 1 | **74.9** | **92.1** |

Table 4: **Effect of adding nearest-neighbors as positives** in various settings. Results are obtained for ImageNet linear evaluation.

| Method | SimCLR [9] | BYOL [25] | NNCLR |
|---|---|---|---|
| Full aug. | 67.9 | 72.5 | 72.9 |
| Only crop | 40.3 (↓ -27.6) | 59.4 (↓ -13.1) | **68.2** (↓ -4.7) |

Table 5: **Performance with only crop augmentation.** ImageNet top-1 performance for linear evaluation is reported.

| Queue Size | 8192 | 16384 | 32768 | 65536 | 98304 |
|---|---|---|---|---|---|
| Top-1 | 73.6 | 74.2 | 74.9 | 75.0 | **75.4** |
| Top-5 | 91.2 | 91.7 | 92.1 | 92.2 | **92.3** |

| $k$ in Top-$k$ NN | 1 | 2 | 4 | 8 | 16 | 32 |
|---|---|---|---|---|---|---|
| Top-1 | **74.9** | 74.1 | 73.8 | 73.8 | 73.8 | 73.2 |
| Top-5 | **92.1** | 91.6 | 91.5 | 91.4 | 91.3 | 91.2 |

| Type of NN | Top-1 | Top-5 |
|---|---|---|
| Soft nearest-neighbor | 71.4 | 90.4 |
| Hard nearest-neighbor | **74.9** | **92.1** |

Dwibedi et al., 2021

# NNCLR: ablations

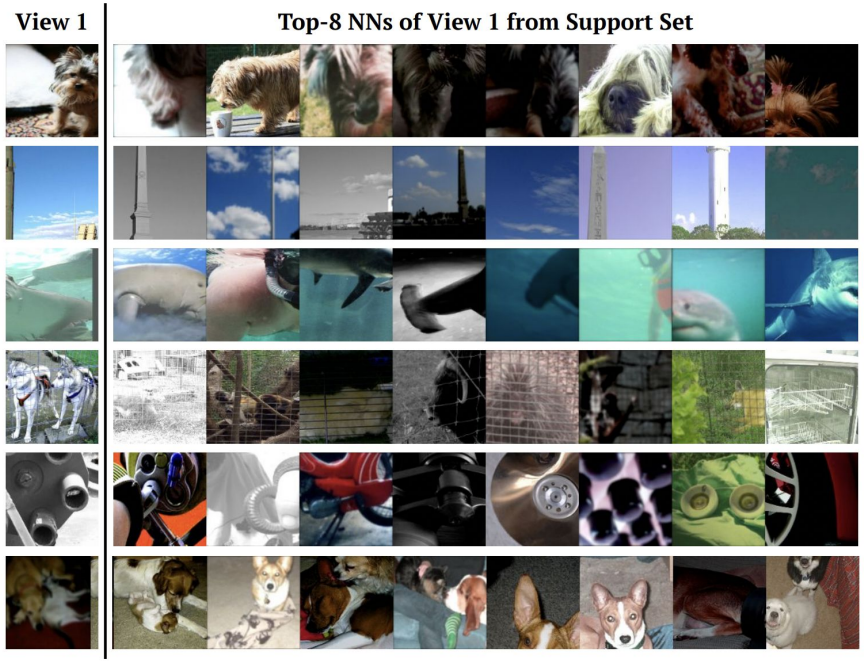


Figure 5: **Nearest neighbors from support set** show the increased diversity of positives in NNCLR.

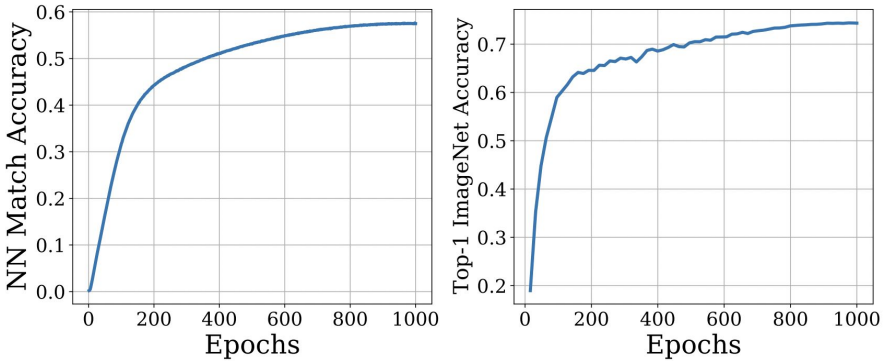


Figure 3: **NN Match Accuracy vs. Performance.**

Dwibedi et al., 2021